Graphene-Based Heat Spreader for Flexible Electronic Devices

Sang-Hoon Bae, Roxana Shabani, Jae-Bok Lee, Seung-Jae Baeck,
Hyoung Jin Cho, and Jong-Hyun Ahn

***Abstract*— Graphene known for its superb physical properties, such as high transparency and thermal conductivity, is proposed as a solution to the problem of thermal management of the electronic devices, requiring transparency and cooling. It is shown that graphene heat spreader layer drives the heat out of the device more efficiently as compared with the commercially used metal thin films for integrated circuit cooling. An application of graphene heat spreader is proposed and tested in chip-on-film packaging. Graphene performance is compared with a gold layer with a similar transparency experimentally and theoretically as a proof of the efficient thermal management capability of graphene.**

***Index Terms*— Chemical vapor deposition (CVD), chip-on-film, graphene, heat spreader, thermal conductivity.**

I. Introduction

OVER the past decades, chip-on-film, also known as chip-on-flex (COF), is widely used as a packaging material for the driver integrated circuit (IC) of color displays [1], [2]. The COF consists of two layers: 1) copper (Cu) and 2) polyimide (PI). The PI layer electrically insulates the active device from the substrate, which causes excessive temperature rise in the driver IC, leading to performance degradation and early thermal breakdowns. Therefore, an efficient thermal management becomes an integral part of the device design to achieve long-term reliability and optimum performance [3]–[6]. One possible solution to dissipate the heat from the localized hot spots is to incorporate a metal thin film such as aluminum, which has a high thermal conductivity of 237 W/mK [7]. However, since metal films are opaque, their application in optical packaging of IC chips on film is restricted [8], [9].

Manuscript received August 21, 2014; revised October 16, 2014; accepted October 20, 2014. Date of publication November 11, 2014; date of current version December 9, 2014. This work was supported in part by the U.S. National Science Foundation under Grant ECCS 1102280 and Grant EEC1343749, in part by the Development Program of Manufacturing Technology for Flexible Electronics with High Performance through the Korea Institute of Machinery and Materials, Daejeon, Korea, under Grant SC0970, and in part by the National Research Foundation of Korea under Grant NRF-2012R1A2A1A03006049 and NRF-2009-0083540. The review of this paper was arranged by Editor R. Venkatasubramanian.

S.-H. Bae, J.-B. Lee, and S.-J. Baeck are with the School of Electrical and Electronic Engineering, Yonsei University, Seoul 120-749, Korea.

R. Shabani and H. J. Cho are with the Department of Mechanical and Aerospace Engineering, University of Central Florida, Orlando, FL 32816 USA (e-mail: hjcho@ucf.edu).

J.-H. Ahn is with the School of Electrical and Electronic Engineering, Yonsei University, Seoul 120-749, Korea (e-mail: ahnj@yonsei.ac.kr).

Color versions of one or more of the figures in this paper are available online at http://ieeexplore.ieee.org.

Digital Object Identifier 10.1109/TED.2014.2364606

Recently, researchers have explored an alternative material, which has a high thermal conductivity as well as a good optical transparency. Graphene, the thinnest elastic material, has superb thermal and optical properties, which makes it a promising material for various applications [10]–[16]. It is reported that thermal conductivity of suspended graphene has an extraordinary value in the range between 2000 and 5000 W/mK at room temperature and in particular, that of suspended graphene grown by chemical vapor deposition (CVD) method exceeded $\sim$2500 W/mK at 350 K [17]–[22]. Recently, Kim *et al.* [23] reported that the thermal conductivity of graphene is saturated to $\sim$1089.6 W/mK due to the interlayer coupling when it is stacked over two layers [23]. For practical applications, it is necessary to transfer graphene to a substrate. The measurements for exfoliated graphene on SiO_2 wafer display $\sim$600 W/mK which is lower than that ($\sim$1089.6 W/mK) of suspended one near room temperature because of strong interface scattering of flexural modes and phonons leaking across the interface between graphene and substrate [24]. This value is still superior to thermal conductivity of common metals such as gold (Au) ($\sim$318 W/mK) and copper (Cu) ($\sim$400 W/mK). Thus, high thermal conductivity of graphene makes it a good candidate material for the thermal management of the electronic devices. In addition, its outstanding optical transmittance ($\sim$97.3%) in company with good thermal property makes it a promising material for electronic systems requiring transparency [25].

In this paper, we demonstrated the possibility of graphene as heat spreaders and suggested a practical application of graphene-based heat spreaders to COF packages, which not only provides good optical transparency, but also corroborates the stability of thermal performance during IC chip operation. The multilayer-stacked graphene on PI film displays a good thermal conductivity approaching to $\sim$600 W/mK at ambient conditions. Beyond having good thermal conductivity values, it also shows optical transparency ($>$65%) in the visible wavelength range, making them suitable for electronic device applications where a combination of both properties is required. We expect both properties can broaden the adaptable range of the heat spreader applications. The proposed graphene heat spreader is also compatible to industrial scale fabrication processes such as roll-to-roll printing.

II. Experiment

$Ni/SiO_2/Si$ substrate was loaded into the chamber. Here, Ni metal layer was used as a catalyst layer to grow

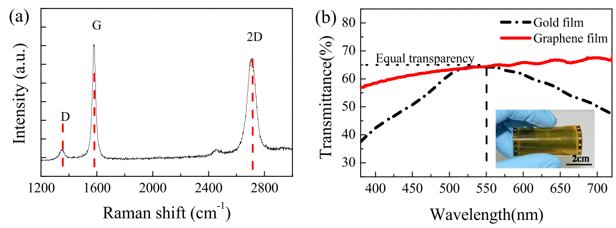

Fig. 1. (a) Raman spectrum of graphene film. The excitation wavelength is 514 nm. A weak D and strong G and 2-D band peaks are shown at 1350, 1580, and 2670 cm^{-1}, respectively. (b) Transmittance spectrums of graphene and gold films (15 nm). The two films have equal transparency at a wavelength of 550 nm.

TABLE I

MATERIAL LAYERS AND THEIR THICKNESSES FOR EACH SAMPLE

Sample #	Detailed Structure information
S1	Serpentine Au(100nm)/Serpentine Cr(3nm)/PET(50um)/PDMS/glass
S2	SU-8(70nm)/Serpentine Au(100nm)/Serpentine Cr(3nm)/PET(50 μm)/PDMS/glass
S3	Graphene/SU-8(70nm)/Serpentine Au(100nm)/Serpentine Cr(3 nm)/PET(50um)/PDMS/glass
S4	1 time stacked graphene(2.5)/COF
S5	2 time stacked graphene(5 nm)/COF
S6	3 time stacked graphene(7.5)/COF
S7	Graphite/COF
S8	Gold(15 nm)/COF

the graphene. After being heated up to 1000 °C, H_2 and Ar, CH_4 gases were flowed into the chamber and reacted for 5 min. During rapid cooling, the graphene film formed on the Ni surface. A Raman spectrum measured to estimate the quality of graphene. Fig. 1(a) indicates that the graphene film has strong G and 2-D bands peaks and a weak D band peak at 1580, 2670, and 1350 cm^{-1}, respectively, which means graphene has suitable quality to be used in the experiment. Fig. 1(b) shows the transmittance of graphene and Au thin films. The Au thin film was used to compare the heat management characteristic of graphene to that of the metal layers because the thermal conductivity of gold is higher than that of the commercially used metal layers such as aluminum (Al) for the thermal management. They have a similar transmittance of 65% at a wavelength of 550 nm, which allows us to compare thermal management properties of both materials [7], [25], [26]. A single layer of graphene reduces the transparency of the film by 2.3%, therefore 65% transmittance of our sample indicates that it is composed of 15 layers of graphene [27]. Here, graphene film was formed using well known CVD method as described above [27], [28]. Before studying the adaptability of graphene to COF, we first needed to understand the heat spreading properties of graphene. For those purposes, a serpentine patterned gold heater was prepared in samples S1 to S3 listed in Table I for this experiment. A 50-μm-thick layer of PET with a width and a length of 1.5×1.5 cm^2 was prepared and a bilayer of chromium (Cr) and Au, with thicknesses of 3 and 100 nm, respectively, were deposited by thermal evaporation (SNTEK, Inc.) onto the PET surface. The Cr was used to enhance Au adhesion to the PET layer [29]. A thin layer of AZ 1512, which is a positive photoresist, was spin-coated on top and patterned in the form of a serpentine,

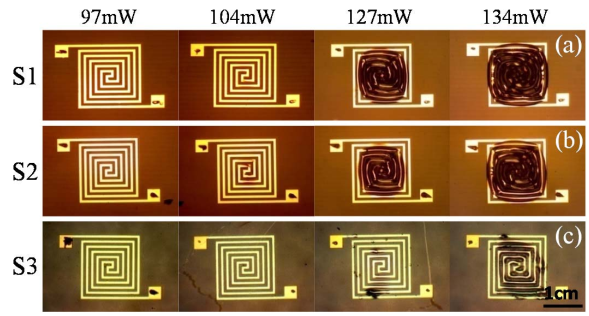

Fig. 2. Microscope images of serpentine gold microheaters on PET substrates which are (a) exposed to air in sample S1, (b) coated with a thin layer of epoxy in sample S2, and (c) coated with a thin layer of epoxy and a graphene film in sample S3. The input power was increased from 97 to 134 mW to compare the heat spreading performances of the samples S1–S3.

using photolithography. The sample was immersed in an Au etchant for 50 s and then Cr etchant for 5 s to remove those parts of the Au–Cr bilayer, which were not protected by the patterned resist. Finally, the AZ 1512 photoresist was removed by acetone followed by rinsing with isopropyl alcohol and deionized water. This method was used to form the gold microheaters in the form of a serpentine in samples S1–S3. The second sample (sample S2) was prepared similar to the first sample and was spin-coated with a thin layer of SU-8 2005 photoresist (Microchem Corp.) with a thickness of 750 nm, to cover the heater structure and provide an electrical insulation. The third sample (sample S3) was prepared similarly to the second sample and covered with a graphene film by transferring graphene on top of the SU8 layer. The two square contact pads were exposed using photolithography and oxygen plasma reactiveion etching, to make the electrical contacts.

III. RESULT AND DISCUSSION

Using those three different samples (S1: Au heater/PET/PDMS/glass, S2: SU-8/Au heater/PET/PDMS/glass, and S3: graphene/SU-8/Au heater/PET/PDMS/glass), the heat spreading performances of each sample were tested by applying an electrical power to the microheaters. An optical microscope was used to monitor the changes in the sample surfaces, whereas the voltage was applied to the electrical contact pads. The sample surfaces did not deteriorate at the powers $<$104 mW. However, those samples, which were not covered by the graphene film (S1 and S2), could not endure the heat generated by a power of $>$104 mW, since their temperatures increased above the degradation temperature of the PET [30]. The microheaters directly exposed to air (S1) seem to be seriously damaged at 127 mW and above [Fig. 2(a)], whereas, the microheaters coated only with the thin epoxy layer (S2) look less affected as compared with that of sample S1 [Fig. 2(b)]. However, the surface of the microheaters covered with a graphene film in the sample S3, was observed to be in a much better condition at the similar input powers [Fig. 2(c)]. Therefore, a graphene film could be used to efficiently spread the heat to avoid thermal damages caused by the increased input power.

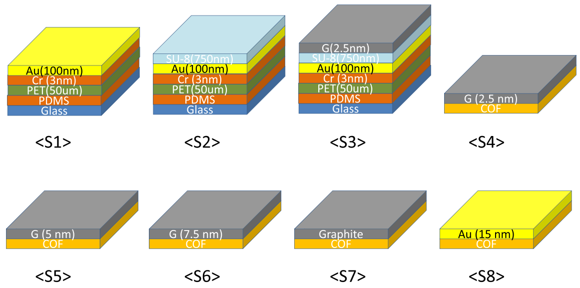

Fig. 3. Diagram for each sample, S1–S8.

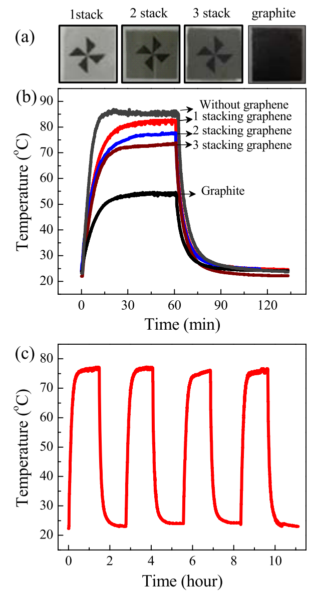

Fig. 4. Hot spot test results. (a) A windmill pattern placed beneath samples S4 to S7 shows decrease in transparency as graphene thickness increases. (b) Temperature versus time measured for different thicknesses of the graphene heat spreader layers. (c) Cyclic test of graphene film on COF film.

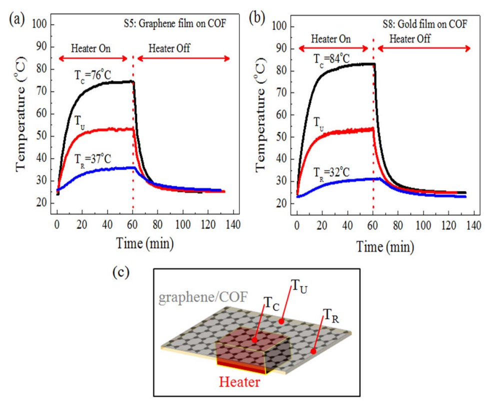

Fig. 5. Hot spot test was performed for samples S5 and S8. (a) Sample S5: graphene film on COF. (b) Sample S8: gold film on COF. (c) Temperatures at three points of center, top, and right, were measured versus time, using three thermocouples.

To adapt the heat spreading effect of graphene to real applications, we prepared several COF samples with various thicknesses of graphene. With those samples, a hot spot test was carried out to find out the effect of the thickness on its heat spreading performance. Graphene film was prepared and transferred on the COF layer using a poly(methyl methacrylate) (PMMA) supporting layer. In more details, graphene film was formed on Ni/SiO_2/Si wafer using the CVD method [27], [28] and transfered to the COF target substrate using PMMA supporting layer. Here, since Ni is used as a catalyst layer, the multilayer graphene was synthesized. We repeated this process and stack another graphene film on top of the sample. The thickness of graphene could be varied by repeating the stacking sequence. The graphene films stacked one time (S4), two times (S5), and three times (S6) were used as well as a graphite film (S7) and the Au thin film (S8) for comparative study (Table I and Fig. 3). The Au was transferred on the COF layer using PMMA and the supporting layer was removed to form sample (S8). Here, the van der Waals force between Au thin film and COF is strong enough to affix Au to COF film.

A heater was placed under the sample and a silicone based heat sink compound was used between them to facilitate the heat transfer to the sample and minimize unexpected heat loss by convection [31], [32]. The temperature of the center point on the sample was measured using a thermocouple to examine the change in the surface temperature of the samples versus time. All temperatures dramatically increased within the first 15 min after the heater was turned on and in the next 45 min, they gradually reached a plateau with a constant value [Fig. 4(b)]. Here, we waited until the temperature became saturated to avoid inaccurate information. The heater was then turned off to let the temperatures drop down to the room temperature. A comparison between the saturation temperatures shows the graphene film's heat spreading performance improves as its thickness increases. This is expected considering the lateral thermal resistance of the graphene layer, $R_t \sim (k_G d_G)^{-1}$, where d_G is thickness of the graphene film, and k_G is its thermal conductivity. The lower the thermal resistance becomes, the more easily the developed heat is carried away. This results in the reduction of the steady-state temperature. However, by increasing the graphene thickness, its transparency is reduced, and as shown in Fig. 4(a), the windmill patterns placed underneath the graphene films in samples S4–S7 become less visible. A graphene film with a thickness of 9 nm (2 times stacked graphene film in sample S5) was selected by considering the two factors of low thermal resistance and high transparency. The hot spot test was repeated several times using this sample to examine the reliability of the heat spreader performance. A similar change in the sample surface temperature was measured in every cycle, which shows the reproducibility of the performance under the thermocycling condition [Fig. 4(c)].

In another experiment, Au film was prepared and transferred on the COF (sample S8 in Table I). The hot spot test was carried out for sample S5 (graphene/COF) and S8 (Au/COF) to understand the heat management performance of the graphene heat spreader, as compared with that of the gold heat spreader [20], [33], [34]. Temperatures of three points on the samples S5 and S8 marked as the center, top, and right, T_C, T_U, and T_R, respectively, were measured using thermocouples to examine the change in the surface temperatures of the samples at different points versus time [Fig. 5(a) and (b)]. The test started by turning on the heater similar to the

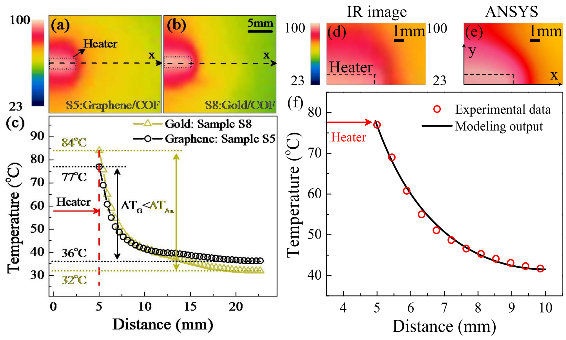

Fig. 6. IR images showing the 2-D temperature distribution of (a) sample S5: graphene heat spreader, (b) sample S8: gold heat spreader in the hot spot test, (c) temperature versus distance along the centerlines of the graphene and gold heat spreaders. A comparison between the modeling and experimental data. (d) IR image of the graphene heat spreader of sample S5 in a hot spot test. (e) 2-D temperature distribution contour of the top view of a model of a quarter of the sample. The x and y axes are the two axes of the symmetry of the problem. (f) Experimental data and modeling result for temperature versus the distance from the center position on the sample along the x-axis.

previous experiment. The temperatures dramatically increased for the first 15 min until leveling off after 60 min The heater was then turned off. The stabilized T_C for graphene heat spreader was lower than that for the gold heat spreader, while the saturated T_R, measured on the edge of the samples [Fig. 5(c)] for graphene heat spreader was higher than that for gold heat spreader.

Therefore, the graphene-based heat spreader is reducing the temperature difference between the center and the edge of the sample for a similar input power, by spreading the heat more efficiently. That is, graphene heat spreaders result in a smaller temperature difference from the center to the edge of the sample. This can be expected due to a very high thermal conductivity of graphene in comparison to that of gold which is comparable to the commercially available metals for heat spreaders such as aluminum. Moreover, while thermal properties of metallic materials may suffer at smaller scales (lower thermal conductivity for thin metal films), due to the surface and grain boundary scattering phenomena, graphene's thermal conductivity is very high in nanoscale thicknesses and therefore could serve as an efficient thin heat spreader whereas thin metal films could not [26]. The temperature distribution of the graphene layer in two-dimension was observed using infrared imaging. Fig. 6(a) and (b) show the IR images taken from the graphene and gold heat spreaders (samples S5 and S8) from top view using an infrared camera. For this IR measurement, a carbon spray was used to keep the emissivity of samples at the level of 0.95%. A comparison between the temperatures on the edge of the two samples, taken from the temperature color code of the IR images, shows that heat has been more evenly spread across the graphene heat spreader. For a more detailed analysis, the surface temperatures of the samples were plotted versus the distance from the center points on the samples along the x-axis. The surface temperature decreases as the distance increases from the edge of the heater to the edge of the sample, as shown in Fig. 6(c). The temperatures of graphene and gold heat spreaders were 77 °C and 84 °C, respectively, at the distance of 5 mm (the heater edge), which gradually decrease by increasing the distance to the edge of the samples. This indicates that the average temperature of graphene heat spreader is lower than that of Au heat spreader. That is, graphene can more effectively spread thermal energy localized in the center area than gold metal film.

To understand the various key factors involved in graphene film on COF and how these can affect the thermal properties, numerical simulations were carried out using a model of the graphene heat spreader and the finite-element analysis software (ANSYS, Inc.), for a quarter of the sample by taking advantage of the symmetry of the problem. A perfectly insulated boundary condition was applied to the two cut surfaces which form new boundaries for the quarter of the sample, since there is no heat transfer across these boundaries due to the symmetry of the problem. A free convection boundary condition with a film coefficient of h, was applied to all surfaces in contact with air. A constant heat flux, q'', boundary condition was applied to the sample surface in contact with the heater. The heat spreader surface temperature is a function of h and q''; therefore, the simulation was done by systematically changing the values of h and q'' to fit the experimental data for temperature versus the distance, x measured along the centerline in a hot spot test. ANSYS calculated h to be 1 $W/m^2 \cdot °C$ and q'' to be 800 W/m^2 for the best fit to the data. For simulation, the PI thermal conductivity of 0.52 W/mK was used as constant, reference value. In case of graphene, it was found that the best value for the closest fit to the experimental data is ~600 W/mK after inputting various values ranging from 400 to 2000 W/mK. In previous reports, thermal conductivity of graphene on SiO_2 substrate decrease to ~600 W/mK and suspended, multilayer graphene is saturated to 1090 W/mK [23], [24]. Multilayer graphene films attached to PI film of COF can exhibit a little different behavior from a flat substrate such as SiO_2 wafer because they can be locally suspended on PI film with rough surface and the effect from the bottom substrate can be attenuated by randomly stacked layers. The fitted value of 600 W/mK seems reasonable one, considering such numerous factors that can affect overall thermal conductivity. As expected q'' was found to be less than the total electrical power of the heater due to the heat loss to the ambient. The 2-D temperature distribution calculated by ANSYS, is in good agreement with the IR image taken from the sample S5 [Fig. 6(d) and (e)]. In addition, the modeling result for temperature versus the distance, x perfectly fits the experimental data measured in the hot spot test [Fig. 6(f)].

IV. Conclusion

Graphene due to its high thermal conductivity and good transparency is an effective heat spreader layer at the reduced scale where the thermal management using conventional metal layers becomes less effective. The hot spot tests verified a smaller temperature variation, i.e., more even temperature distribution between the heated center and the edge when graphene is used as a heat spreader layer as compared with a gold layer. An optimum thickness for graphene was obtained by taking into account of two important parameters: 1) high transparency and 2) low thermal resistance. The comparative study in this paper shows that graphene could be used for thermal management in repeated thermocycles with no apparent degradation. In addition, a simple additive fabrication process can be easily adopted to various chip-on-film applications for the effective thermal management where cooling is critical to device performances.

REFERENCES

[1] A. Sugimoto, H. Ochi, S. Fujimura, A. Yoshida, T. Miyadera, and M. Tsuchida, "Flexible OLED displays using plastic substrates," *IEEE J. Sel. Topics Quantum Electron.*, vol. 10, no. 1, pp. 107–114, Jan./Feb. 2004.

[2] W.-C. Kao, J.-A. Ye, F.-S. Lin, P.-Y. Cheng, and R. Sprague, "Configurable timing controller design for active matrix electrophoretic display," *IEEE Trans. Consum. Electron.*, vol. 55, no. 1, pp. 1–5, Feb. 2009.

[3] T.-H. Kim *et al.*, "Printable, flexible, and stretchable forms of ultrananocrystalline diamond with applications in thermal management," *Adv. Mater.*, vol. 20, no. 11, pp. 2171–2176, Jun. 2008.

[4] I. Mudawar, "Assessment of high-heat-flux thermal management schemes," *IEEE Trans. Compon. Packag. Technol.*, vol. 24, no. 2, pp. 122–141, Jun. 2001.

[5] L.-T. Yeh and R. C. Chu, *Thermal Management of Microelectronic Equipment: Heat Transfer Theory, Analysis Methods and Design Practices*. New York, NY, USA: ASME, 2002.

[6] M. Mahalingam, "Thermal management in semiconductor device packaging," *Proc. IEEE*, vol. 73, no. 9, pp. 1396–1404, Sep. 1985.

[7] E. H. Hollingsworth and H. Y. Hunsicker, "Corrosion resistance of aluminum alloys in metals handbook," in *Proc. Amer. Soc. Met.*, vol. 2. Metals Park, OH, USA, 1979, p. 204.

[8] A. Christensen, M. Ha, and S. Graham, "Thermal management methods for compact high power LED arrays," in *Proc. SPIE, 7th Int. Conf. Solid State Lighting*, vol. 6669. San Diego, CA, USA, Sep. 2007, pp. 66690Z-1–66690Z-19.

[9] A. Bar-Cohen, "Thermal management of air- and liquid-cooled multichip modules," *IEEE Trans. Compon., Hybrids, Manuf. Technol.*, vol. 10, no. 2, pp. 159–175, Jun. 1987.

[10] S.-K. Lee *et al.*, "All graphene-based thin film transistors on flexible plastic substrates," *Nano Lett.*, vol. 12, no. 7, pp. 3472–3476, Jul. 2012.

[11] T.-H. Han *et al.*, "Extremely efficient flexible organic light-emitting diodes with modified graphene anode," *Nature Photon.*, vol. 6, pp. 105–110, Jan. 2012.

[12] Z. Liu *et al.*, "Organic photovoltaic devices based on a novel acceptor material: Graphene," *Adv. Mater.*, vol. 20, no. 20, pp. 3924–3930, Oct. 2008.

[13] S.-H. Bae, Y. Lee, B. K. Sharma, H.-J. Lee, J.-H. Kim, and J.-H. Ahn, "Graphene-based transparent strain sensor," *Carbon*, vol. 51, pp. 236–242, Jan. 2013.

[14] S.-H. Bae *et al.*, "Graphene-P(VDF-TrFE) multilayer film for flexible applications," *ACS Nano*, vol. 7, no. 4, pp. 3130–3138, Feb. 2013.

[15] J. Kim, V. C. Tung, and J. Huang, "Water processable graphene oxide: Single walled carbon nanotube composite as anode modifier for polymer solar cells," *Adv. Energy Mater.*, vol. 1, no. 6, pp. 1052–1057, Nov. 2011.

[16] V. C. Tung, J.-H. Huang, J. Kim, A. J. Smith, C.-W. Chu, and J. Huang, "Towards solution processed all-carbon solar cells: A perspective," *Energy Environ. Sci.*, vol. 5, no. 7, pp. 7810–7818, Apr. 2012.

[17] E. Pop, V. Varshney, and A. K. Roy, "Thermal properties of graphene: Fundamentals and applications," *MRS Bull.*, vol. 37, no. 12, pp. 1273–1281, Dec. 2012.

[18] A. A. Balandin *et al.*, "Superior thermal conductivity of single-layer graphene," *Nano Lett.*, vol. 8, no. 3, pp. 902–907, Feb. 2008.

[19] S. Berber, Y.-K. Kwon, and D. Tománek, "Unusually high thermal conductivity of carbon nanotubes," *Phys. Rev. Lett.*, vol. 84, no. 20, pp. 4613–4616, May 2000.

[20] S. Ghosh *et al.*, "Extremely high thermal conductivity of graphene: Prospects for thermal management applications in nanoelectronic circuits," *Appl. Phys. Lett.*, vol. 92, no. 15, p. 151911, Apr. 2008.

[21] W. Cai *et al.*, "Thermal transport in suspended and supported monolayer graphene grown by chemical vapor deposition," *Nano Lett.*, vol. 10, no. 5, pp. 1645–1651, Apr. 2010.

[22] M.-H. Bae *et al.*, "Ballistic to diffusive crossover of heat flow in graphene ribbons," *Nature Commun.*, vol. 4, pp. 1–7, Apr. 2013, Art. ID 1734.

[23] D. Kim, Y. Hwangbo, L. Zhu, A. E. Mag-Isa, K.-S. Kim, and J.-H. Kim, "Dimensional dependence of phonon transport in freestanding atomic layer systems," *Nanoscale*, vol. 5, no. 23, pp. 11870–11875, Dec. 2013.

[24] J.-H. Seol *et al.*, "Two-dimensional phonon transport in supported graphene," *Science*, vol. 328, no. 5975, pp. 213–216, Apr. 2010.

[25] R. R. Nair *et al.*, "Fine structure constant defines visual transparency of graphene," *Science*, vol. 320, no. 5881, p. 1308, Apr. 2008.

[26] G. Chen and P. Hui, "Thermal conductivities of evaporated gold films on silicon and glass," *Appl. Phys. Lett.*, vol. 74, no. 20, p. 2942, Mar. 1999.

[27] S. Bae *et al.*, "Roll-to-roll production of 30-inch graphene films for transparent electrodes," *Nature Nanotechnol.*, vol. 5, pp. 574–578, Mar. 2010.

[28] K. S. Kim *et al.*, "Large-scale pattern growth of graphene films for stretchable transparent electrodes," *Nature*, vol. 457, pp. 706–710, Feb. 2009.

[29] N. R. Moody, D. P. Adams, D. Medlin, T. Headley, N. Yang, and A. Volinsky, "Effects of diffusion on interfacial fracture of gold–chromium hybrid microcircuit films," *Int. J. Fract.*, vol. 119, nos. 1–2, pp. 407–419, Jan. 2003.

[30] E. W. H. Jager, E. Smela, and O. Inganäs, "Microfabricating conjugated polymer actuators," *Science*, vol. 290, no. 5496, pp. 1540–1545, Nov. 2000.

[31] G. K. White, "The thermal conductivity of gold at low temperatures," *Proc. Phys. Soc., Sec. A*, vol. 66, no. 6, pp. 559–564, Jun. 1953.

[32] D. D. L. Chung, "Thermal interface materials," *J. Mater. Eng. Perform.*, vol. 10, no. 1, pp. 56–59, Feb. 2001.

[33] S. Chen *et al.*, "Thermal conductivity of isotopically modified graphene," *Nature Mater.*, vol. 11, pp. 203–207, Jan. 2012.

[34] Z. L. Wu, P. K. Kuo, W. Lanhua, S. L. Gu, and R. L. Thomas, "Photothermal characterization of optical thin films," *Thin Solid Films*, vol. 236, nos. 1–2, pp. 191–198, Dec. 1993.

Jong-Hyun Ahn received the Ph.D. degree from the Pohang University of Science and Technology, Pohang, Korea, in 2001.

He is currently a Professor with the School of Electrical and Electronic Engineering, Yonsei University, Seoul, Korea. His current research interests include production of graphene and 2-D materials, and their application in flexible electronics.

Hyoung Jin Cho received the B.S. and M.S. degrees in materials engineering from Seoul National University, Seoul, Korea, in 1991 and 1989, respectively, and the Ph.D. degree in electrical engineering from the University of Cincinnati, Cincinnati, OH, USA, in 2002.

He is currently a Professor with the Department of Mechanical and Aerospace Engineering, University of Central Florida, Orlando, FL, USA.